

Pattern Width Description through Disk Cover

Application to Digital Font Recognition

Nikita Lomov and Leonid Mestetskiy

*Moscow State University, Faculty of Computational Mathematics and Cybernetics, Moscow, Russia
{nikita-lomov, mestlm}@mail.ru*

Keywords: Disk Cover, Morphological Width, Polygonal Figure, Medial Representation, Skeleton, Radial Function, Bicircle, Font Comparing.

Abstract: We consider the concept of "the width of a figure" for objects of complex shapes in order to use it as an integral morphological descriptor in image recognition tasks. In this article we propose a new approach to the description of this concept on the basis of the figures covering by disks of a certain size. The area of the disk cover as a function of the covering disc size is a shape descriptor. Original method for analytical calculation the area of disk cover of polygonal shapes is presented. The method is universal because there is always the possibility of polygonal approximating of complex digital binary images and geometric objects with nonlinear boundary. The method is based on the medial representation of the polygonal figure as a skeleton and a radial function. Our approach ensures high accuracy and computational efficiency calculate the area of disk cover. The effectiveness of the proposed approach is demonstrated for applications in computer font's recognition problem.

1 INTRODUCTION

The width of the objects is an important feature of image shape. This feature cannot be well described by a scalar value, such as "average" width, for the objects of complex shape, in which the different parts have different width and length. Therefore, the description of width "distribution" that characterizes the whole range of its values is required to be used as width descriptor.

Local description of the width can be based on the size of the primitive, which can be inscribed in the object. The larger width of the object, the larger the size of the primitive. If we inscribe in the object the primitives of a given size, such as disks of a certain diameter, the part of the object covered by the primitives can be considered as a region of a given width. Then the function describing the dependence of the region area from the primitive size can be regarded as an integral description of the object width. This article proposes an approach to the construction of the image width descriptor, which is based on the area of the disk cover of the object (Fig.1). Selecting a disk as primitive provides invariance of the descriptor to the shift, rotation and scaling of images.

The object width descriptor is a diagram representing the dependency of the cover area from the size of covering disks (Fig.2).



Figure 1: Disk covers of the "lizard" figure (on the right the examples of covering disks are shown).

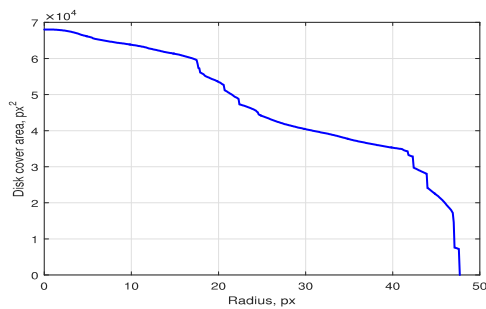


Figure 2: Diagram of the dependency of disk cover area of the “lizard” figure from the size (radius) of covering disks.

To compute the cover area, the method of pattern spectrum (Maragos, 1989), based on a discrete mathematical morphology (Serra, 1982), can be applied. In this case, the object width descriptor is the pattern spectrum diagram, constructed on the base of morphological opening operation using a disc structuring element. An example of this approach is described in (Ramirez-Cortes et al., 2008). Pattern spectrum method allows a simple software implementation, however, it has a high computational complexity, especially when working with large high-resolution images. To cope with this problem in (Vizilter and Sidiyakin, 2012, 2014) a combined discrete-continuous approach to the calculation of the pattern spectrum was proposed, which allowed significantly reduce the computation time, but not so much. The task cannot be solved in real-time of the computer vision systems.

Our approach is aimed at drastically reducing the computation time of the cover area through the use of a continuous model of an image shape. Continuous model is a polygonal shape approximating a digital image. Selecting a polygonal shape (a polygon with polygonal holes) as a model of the object shape is due to two reasons. On the one hand, polygonal shapes can accurately approximate the boundary of complex objects represented by discrete raster images. On the other hand, for the polygonal figure the regions of a given width can be described using the medial representation – the skeleton and the radial function. A medial representation of a polygonal shape can be obtained with high-performance computational geometry algorithms (Mestetskiy, 2008).

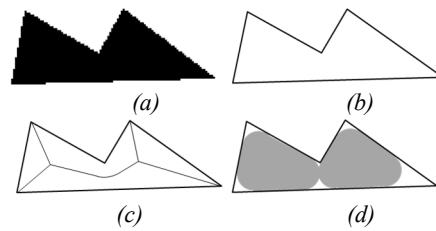


Figure 3: Continuous model of the disk cover for binary image: a) binary image, b) approximating polygonal figure c) its skeleton, d) example of r-cover.

Our method of the calculation of the disk cover area for objects on bitmap images includes the following steps:

1. Approximation of a binary image by a polygonal shape.
2. Medial representation of a polygonal shape in the form of the skeleton and the radial function based on Voronoi diagrams of line segments that constitute the shape boundary.
3. Representation of a complex-shaped polygonal figure as a union of bicircles – elementary geometric shapes corresponding to the edges of the skeleton.
4. Representation of the figure disk cover as the union of a subset of bicircles and calculating the cover area through bicircles' areas.
5. Construction of the distribution function of the disk cover area as a function of the disk size.

2 DISK COVER AND FIGURE SKELETON

Definition 1. A figure is a closed region in the plane bounded by a finite number of disjoint closed Jordan curves.

Definition 2. A circle is considered to be empty if it is located entirely in the figure.

Definition 3. Disk r -cover of the figure is the union of all empty circles of the radius r . Examples of disk r -cover for different values of r are shown in Fig.1.

Definition 4. r -area of the figure is the area of its disk r -cover.

According to this definition, the area of the entire figure is its 0-area.

Definition 5. Morphological width $F(r)$ of the figure is its r -area as a function of r . Morphological width is a non-increasing function of the r .

Morphological width could be calculated by using pattern spectrum (Maragos, 1989) through the

opening operation of a discrete mathematical morphology (Serra, 1982). The disk is used as a primitive. This approach requires a lot of computation time, and may be applied only to discrete images. Our method is much faster and is more universal because it allows you to work with discrete and continuous images through approximation by polygonal figure.

Definition 6. An inscribed circle of the figure is an empty circle, which is the maximum, i.e., is not contained in any other empty circle.

Definition 7. A skeleton of a figure is the set of all points that are centers of inscribed circles.

Definition 8. The radial function is defined in the skeleton points and assigns to the skeleton point the radius of the inscribed circle centered at this point.

Obviously, each empty circle of radius more than r can be represented as the union of empty circles of radius r . Therefore, any inscribed circle with radius r or more is contained in the disk r -cover. Consequently, the disk r -cover of the figure coincides with the union of all the inscribed circles of radius at least r . The centers of the inscribed circles constitute a subset of the skeleton points. Thus, for calculating the morphological width of the figure it is sufficient to consider only the circles whose centers lie on the skeleton. The challenge is to obtain for given values of argument r the corresponding values of figure r -area. The solution to this problem for the polygonal shapes will be obtained in an explicit form.

3 POLYGONAL FIGURES AND BICIRCLES

Definition 9. A polygonal figure is a figure whose boundary consists of closed polylines.

The boundary of a polygonal figure can be represented as the union of a finite number of subsets, called sites: point-sites (vertices of the figure) and segment-sites (sides of the figure without end points).

A skeleton of a polygonal figure (Fig.4) looks like geometric graph whose edges are segments of straight lines and quadratic parabolas, and the vertices are the endpoints of edges. Each edge is a connected set of points that are centers of inscribed circles having the same incident pair of sites, called site-generators of the edge. If both site-generators are of the same type (two point-sites or two segment-sites) then the edge is a straight line

segment. If site-generators are of different types (point-site and segment-site) then the edge is a segment of a quadratic parabola.

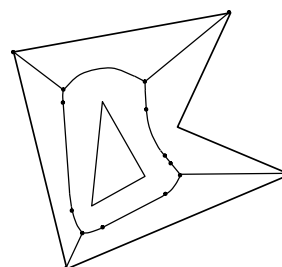


Figure 4: Polygonal figure and its skeleton.

Polygonal approximation of the digital binary image and the construction of the continuous skeleton and radial function are performed by means of high-performance algorithms (Mestetskiy, 2008). The proposed method for calculating r -area, using the special properties of a skeleton of a polygonal shape, is based on the decomposition of the figure on the constituent elements – bicircles.

Definition 10. A bicircle is the union of all inscribed circles centered on one edge of the skeleton. The edge line is called the axis of the bicircle.

Three types of bicircles are distinguished depending on the pair of their site-generators: linear (two segment-sites – Fig.5a-b), parabolic (segment-site and point-site – Fig.5c) and hyperbolic (two point-sites – Fig.5d). This terminology is caused by the dependency of the radial function on the position of a point on the axis of the bicircle.

Circles with centers at the vertices of the skeleton are called the end circles of the bicircle. The boundary of the bicircle is the envelope of the family of its constituent circles. The boundaries of linear and parabolic bicircles include, fully or partially, their generating segment-sites (Fig.5a-c). In addition, the boundaries of all kind of bicircles contain arcs of end circles.

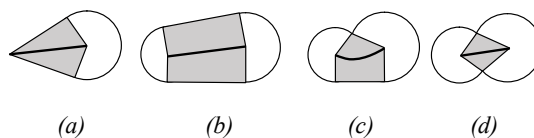


Figure 5: Bicircles: axes, proper regions, external sectors of end circles.

Definition 11. The sector of end circle relied on the arc of the bicircle boundary is called an external sector of a bicircle.

Definition 12. A spoke is a line segment connecting the skeleton point with the nearest point of figure boundary.

Definition 13. A proper region of a bicycle is the union of all spokes of the bicircle incident to points of its axis.

The bicircle is the union of its proper region and the pair of external sectors. The shape of the proper area depends on the type of bicircle (Fig.5). For a linear bicycle it is the union of two triangles (Fig.5a) or two trapezoids (Fig.5b). In the parabolic bicircle it is a “house-shaped” figure, which can be regarded as the union of a trapezoid and a triangle (Fig.5c), in the hyperbolic one it is the union of two triangles (Fig.5d).

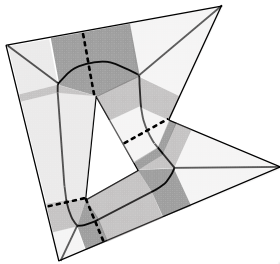


Figure 6: Coverage of the polygonal figure by proper regions of bicircles.

Let M is a polygonal figure, M_r is a subset of the figure formed by the union of all spokes of length r and more. It is obvious that M_r is entirely contained in r -cover. Proper areas of bicircles form the cover of the whole polygonal figure, the cover coincides with the union of all spokes, i.e. $M_0 = M$ (Fig.6).

Definition 14. Bicircle is called monotonic if the radial function monotonically decreases or increases along its axis.

It is clear that a linear bicircle is monotonic, because the linear radial function is monotonic on the axis. A linear bicircle of constant width considered to be monotonic by definition.

In the parabolic bicircle, if the vertex of the parabola is an interior point of the bicircle axis, when passing through the vertex the behavior of the radial function changes from the decreasing to the increasing (Fig.5c). The vertex of the parabola is a point of local minimum of the radial function and the bicycle at this time is not monotonic. In other cases, when the vertex of the parabola lies outside the axis or coincides with the end point of the axis, the parabolic bicircle is monotonic.

In the hyperbolic bicircle, the monotonic property is determined by the position of the centers of end circles with respect to the site line (the line passing through the point-sites). If the centers are on

different sides of this line, the point of intersection of this line with the bicircle axis is inside the axis and the minimum of radial function is achieved in this point – therefore, the bicircle is not monotonic (Fig. 5d). In other cases, the hyperbolic bicircle is monotonic.

Calculation of morphological width for monotonic bicircles involves a simpler problem than for non-monotonic ones. Therefore each non-monotonic bicircle can be replaced with a pair of monotonic ones. So its axis can be divided into two monotonic segments by adding vertices in the bicircles’ minimal points and splitting the respective edges into two parts. In the example (Fig.6) four extreme bicircles are divided into monotonic pairs. The dotted line shows the corresponding proper areas of the bicircles.

4 PROPER REGIONS AND EXTERNAL SECTORS

Figure 6 presents the monotonic bicircles of all three types. Here, r and R are the radii of the small and the large end circles, l is the distance between their centers. If the bicircle is linear or parabolic, it has the generating segment-site, and then t is the length of the projection of the bicycle axis at this site:

$$t = \sqrt{l^2 - (R - r)^2}.$$

In the parabolic bicircle p is the distance between the point-site and a line of the segment-site (the focal parameter of the parabola). In the hyperbolic bicircle q is the distance between point-sites.

For the linear bicircle (Fig.7a) the proper region area is determined as the sum of the areas of two trapezoids, with the bases r and R and the height t :

$$S_{lin} = 2 \cdot \frac{R+r}{2} \cdot t = (R + r) \cdot t. \quad (1)$$

The angular size of the external sector of the small end circle is

$$\varphi_{lin} = 2\alpha = 2 \cdot \arcsin \frac{t}{r}. \quad (2)$$

For parabolic bicircle (Fig.7b) the proper region area is composed of the area of the same trapezoid and the area of the triangle with vertices at the centers of end circles and at the point-site. The area of the triangle is calculated by Heron's formula:

$$S_{par} = \frac{R+r}{2} \cdot t + \sqrt{P(P-R)(P-r)(P-l)}, \quad (3)$$

where $P = (R + r + l)/2$.

The angular size of the external sector of the small end circle of parabolic bicircle is

$$\varphi_{par} = \frac{\pi}{2} + \alpha = \frac{\pi}{2} + \arcsin \frac{p-r}{r}. \quad (4)$$

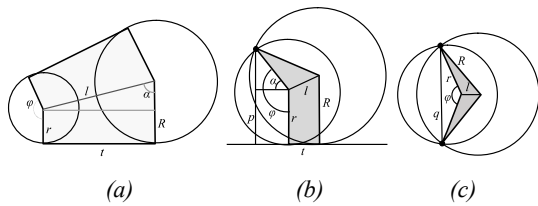


Figure 7: Proper regions and external sectors of bicircles: (a) linear, (b) parabolic, (c) hyperbolic.

Proper region area of the hyperbolic bicircle (Fig.7c) is the sum of the areas of the two triangles, calculated according to Heron's formula:

$$S_{hyp} = 2\sqrt{P(P-R)(P-r)(P-l)}. \quad (5)$$

The angular size of the external sector of the small end circle is

$$\varphi_{hyp} = 2 \arcsin \frac{q}{2r}. \quad (6)$$

5 TRUNCATED BICIRCLES

Disk r -cover of the polygonal figure at $r = 0$ coincides with the polygonal figure. As r increases, the cover shrinks and the part of the figure, covered with disks, diminishes (Fig.8). This cover is a figure whose boundary consists of line segments and arcs.

Disk r -cover is the union of circles with a radius greater than or equal to r , inscribed in the polygonal figure. We call the set of the centers of these circles the axis of the r -cover. Obviously, the axis of the r -cover is the subset of the polygonal figure skeleton. This subset is connected at small values of r , but as r increases it can split into several connected components (Fig.8).

Therefore, the polygonal figure skeleton is divided into two parts: r -cover axis – the subset where the radial function is equal to r or more, and the rest – the subset where the radial function is less than r . Both of these subsets can be considered as geometric graphs.

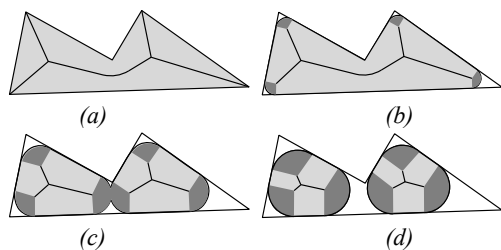


Figure 8: Changing of disk r -cover with increasing disk radius.

For $r > 0$, all bicircles of the polygonal figure are broken down into three groups: wide (all the circles of the bicircle belongs to the r -cover completely), narrow (no circle belongs completely), and truncated (part of the circles belong completely).

Let R_1 and R_2 are the minimum and the maximum radii of circles in the monotonic bicircle. Then $R_1 \geq r$ in the wide bicircle, and $R_2 < r$ in the narrow bicircle.

If $R_1 < r \leq R_2$, then the r -cover includes only those circles of the bicircle, whose radius is not less than r . We define the *truncation* operation of such bicircle, which is to remove the circles with a radius smaller than r . The resulting new bicircle will be called *truncated*. The minimum circle of the truncated bicycle changes to the circle of radius r , and the maximum one remains the circle with a radius R_2 .

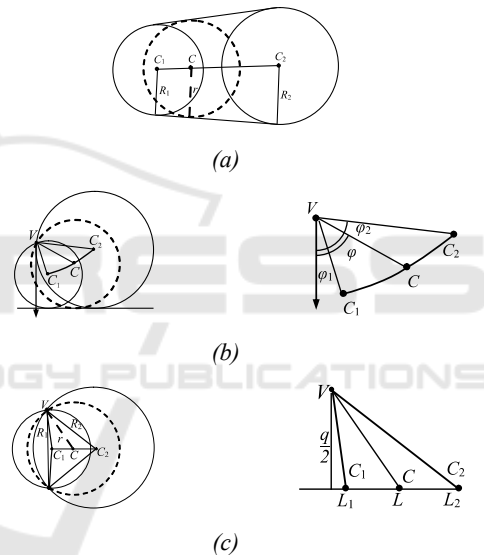


Figure 9: Correction of truncated bicircles.

Let C_1, C_2 are the centers of the small and the great end circles. We determine the new position of the small end circle. Let the point C is the desired center of the circle with radius r (Fig.9).

For the linear bicircle (Fig.9a), we have $C = C_1 + (C_2 - C_1) \cdot \lambda$, where $\lambda = \frac{r-R_1}{R_2-R_1}$. In the particular case when $R_2 = R_1$, we suppose $\lambda = 0$.

For the parabolic bicircle (Fig.9b) choose a polar coordinate system (ρ, φ) with the origin at the point-site V of the bicircle and the axis orthogonal to the segment-site. The equation of the parabola in these coordinates is $\rho = \frac{p}{1+\cos(\varphi)}$, where p is the focal parameter of the parabola. The end circles centers

have coordinates $C_1(R_1, \varphi_1)$ and $C_2(R_2, \varphi_2)$, where $\varphi_1 = \arccos\left(\frac{p}{R_1} - 1\right)$, $\varphi_2 = \arccos\left(\frac{p}{R_2} - 1\right)$. The required point is $C(r, \varphi)$, $\varphi = \arccos\left(\frac{p}{r} - 1\right)$. Without loss of generality, we assume $\varphi_1 < \varphi_2$. Vector \overline{VC} is obtained through rotating $\overline{VC_1}$ by angle $\theta = \varphi - \varphi_1$ and multiplying by factor $\frac{r}{R_1}$. Then the desired center of the circle is $C = V + \frac{r}{R_1} \cdot \mathbf{G} \cdot \overline{VC}$, where \mathbf{G} is the rotation matrix by angle θ :

$$\mathbf{G} = \begin{pmatrix} \cos \theta & -\sin \theta \\ \sin \theta & \cos \theta \end{pmatrix}.$$

In the hyperbolic bicircle (Fig.9c) the point C lies between C_1 and C_2 . Let q is the distance between point-sites. If V is a point-site, the projections of the vectors \overline{VC} , $\overline{VC_1}$, $\overline{VC_2}$ on the bicircle axis have lengths

$$L = |\overline{VC}| = \sqrt{r^2 - \left(\frac{q}{2}\right)^2},$$

$$L_1 = |\overline{VC_1}| = \sqrt{R_1^2 - \left(\frac{q}{2}\right)^2},$$

$$L_2 = |\overline{VC_2}| = \sqrt{R_2^2 - \left(\frac{q}{2}\right)^2}.$$

Then $C = C_1 + (C_2 - C_1) \cdot \lambda$, where $\lambda = \frac{L-L_1}{L_2-L_1}$.

These formulas allow us to find a new position of the small end circle, then the calculation of the area of the bicircle and the angular sizes of the external sectors is carried out by the same formulas (1)–(6), as for wide bicircles.

Therefore, the disk r -cover is the union of two sets of bicircles: full bicircles, where $R_{min} \geq r$, and truncated bicircles, where $R_{min} < r \leq R_{max}$. This cover is composed from proper regions of these bicircles and external sectors of small circles of the truncated bicircles.

At Figure 8 proper regions are highlighted in light gray, and the external sectors – in dark gray. The total area of the union of the proper regions is the sum of areas of bicircles' proper regions.

End circles of truncated bicircles in the r -cover have a radius r . The area of the external sector with an angle φ is $S_{sec} = \frac{\varphi}{2} \cdot r^2$. But the sectors can have a nontrivial intersection (Fig.8c).

6 BICIRCLES' INTERSECTIONS

Define those of the bicircles, which can have significant intersections with each other. When calculating r -area it is only necessary to find the intersections of adjacent bicircles, i.e. those between

which gaps are formed by removing narrow bicircles having a width smaller than r .

We are interested in only the external sectors of the small end circles of the bicircles. In the monotonic bicircle the angular size of the external sectors of the small end circle $\varphi \leq \pi$.

Definition 15. Two truncated bicircles in the r -cover called adjacent if there is a route in the skeleton connecting the centers of the end circles, such that the radial function at all points of the route is less than r .

The external sector of the truncated bicircle may have the intersection not only with the external sector of another bicycle, but also with its proper region. Figure 9 shows examples of possible mutual arrangements of the external sectors of the two truncated bicircles. In the first case (Fig.10a) in the intersection of two sectors the “lens” figure, the boundary of which consists of two equal circular arcs, is formed. In the second case (Fig.10b) the intersection of the sectors is a more complex figure whose boundary includes straight-line segments of the spokes and the circular arcs. The gray highlighted areas in Figure 10 are formed by the union of the external sectors except for the intersection of them with the proper areas of the bicircles. Such areas will be called the outer zone of the bicircle pair.



Figure 10: Mutual arrangement of the pair of crossing external sectors of truncated bicircles.

We denote:

S_{disk} is the area of the end circles of the bicircles;

S_{lens} is the area of the lens formed by the intersection of the end circles;

$S_1^{(ext)}$, $S_2^{(ext)}$ are the areas of the bicircles' external sectors;

$S_1^{(int)}$, $S_2^{(int)}$ are the areas of internal sectors of the end circles.

Internal sector is the addition of the external sector in the end circle. Internal sectors of two adjacent truncated bicircles do not intersect each other. Since the angular size of the external sector does not exceed π , it turns out that the internal sector size is not less than π .

The area of the outer zone formed by a pair of external sectors of the two intersecting truncated

bicircles is the sum of the areas of these sectors less the area of the lens formed by the intersection of the end circles:

$$S = S_1^{(ext)} + S_2^{(ext)} - S_{lens}. \quad (7)$$

Indeed, the total area of the union of two intersecting end circles is equal to

$$2S_{disk} - S_{lens}.$$

Since internal sectors of the circles do not intersect:

$$S = (2S_{disk} - S_{lens}) - (S_1^{(int)} + S_2^{(int)}).$$

Obviously,

$$S_{disk} = S_1^{(ext)} + S_1^{(int)} = S_2^{(ext)} + S_2^{(int)}.$$

Taking this into account, we obtain the desired relation to the area of the outer zone:

$$\begin{aligned} S &= (S_{disk} - S_1^{(int)}) + (S_{disk} - S_2^{(int)}) - S_{lens} = \\ &= S_1^{(ext)} + S_2^{(ext)} - S_{lens}. \end{aligned}$$

Let φ_1, φ_2 are the angular sizes of two intersecting external sectors. Then

$$S_1^{(ext)} = \frac{\varphi_1 \cdot r^2}{2}, \quad S_2^{(ext)} = \frac{\varphi_2 \cdot r^2}{2}.$$

The angular size of the lens formed by the two circles of radius r , with centers located at a distance $h < 2r$ of each other, is

$$\theta = \arccos \frac{h}{2r}.$$

The area of this lens is

$$S_{lens} = r^2(\theta - \sin \theta).$$

Thus, the area (7) of the outer zone of the pair of intersecting bicircles is equal to

$$S = \frac{\varphi_1 \cdot r^2}{2} + \frac{\varphi_2 \cdot r^2}{2} - r^2(\theta - \sin \theta). \quad (8)$$

The case of three or more intersecting external sectors seems more difficult. Possible options for the intersection of three equal circles are depicted in Figure 11.

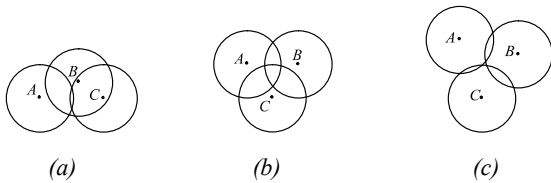


Figure 11: Intersections of three end circles of the truncated bicircles.

However, as shown in (Lomov and Mestetskiy, 2016), in the case of the intersection of three truncated bicircles options shown in Figure 11a,b are impossible. The only possible option for the intersection of three truncated bicircles is pairwise intersections as in the example on Figure 11c.

Consequently, the area of the outer zone formed by the external sectors of three pairwise intersecting truncated bicircles, is the sum of the areas of these sectors minus the areas of lenses

formed by the intersection of end circles. The area of the disk cover is the sum of areas of proper regions of all bicircles and areas of external sectors of the truncated bicircles minus the areas of intersections of adjacent truncated bicircles.

Search for the pairs of adjacent truncated bicircles is performed on the base of the polygonal figure skeleton, starting from the minimum points of the radial function. As a result of the sequential analysis of width of these bicircles, we find all truncated bicircles, bordering the narrow component of the skeleton, adjacent to the given minimum point of the radial function.

7 STRUCTURE OF THE ALGORITHM

Thus, to calculate the r -area we can use the representation of the disk r -cover as the union of bicircles. To do this, take the following steps:

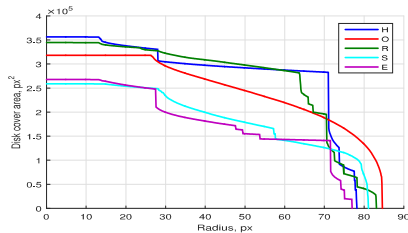
1. Build the medial representation of a polygonal figure in the form of a skeleton and a radial function. The algorithm described in (Mestetskiy, 2008).
2. Find the edges, in which the minimum points of the radial function are located, and divide them down into monotonic parts (Section 3). Build the set of monotonic bicircles covering the polygonal figure.
3. For a given value of r find the set of truncated bicircles and calculate the positions of their small end circles (Section 5).
4. For complete and truncated bicircles calculate the areas of proper regions and take their sum (Section 4).
5. For truncated bicircles determine their external sectors and find their total area (Section 5).
6. Find all the lenses in the intersections of the external sectors and calculate their total area (Section 6).
7. Find the r -area as the sum of areas of proper regions and end sectors of the bicircles minus the total area of the lens.

8 COMPUTER FONT RECOGNITION

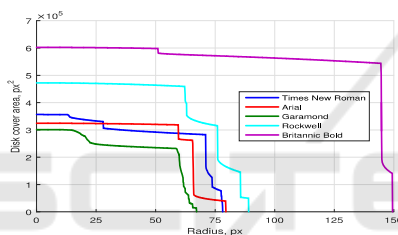
As an example of the proposed method of morphological image analysis we consider the problem of computer font recognition by some

context. Currently, thousands of computer fonts developed. The need to identify what font is used in the text arises for designers, font developers and copyright holder companies. The aim of the experiment is to evaluate the possibilities of using the proposed method for solving these problems.

Example (Fig.12a) demonstrates width diagrams for 5 letters of the Times New Roman font, belonging to the word HORSE. The example shows that the font characters have clearly distinguishable individual portraits.



(a)



(b)

Figure 12: Width diagrams of different characters of the same font (a) and the same character in different fonts (b).

Differences between the portraits of the same letter H, typed by different fonts (Times New Roman, Aria, Garamond, Britannic Bold, Rockwell) are shown in next example (Fig.12b). These diagrams are obtained for high-resolution images, which are considered as reference samples.

To conduct the experiment under more realistic conditions, reference images of 52 characters of the Latin alphabet (26 uppercase and 26 lowercase letters) for 1848 typefaces ParaType digital font collection (Yakupov et al., 2015) have been constructed. For the reference images the width diagrams were obtained by the method described in this article. To do this, each character was drawn on a binary raster image on such a scale that the height of a capital letter H was 1000 pixels. For these images continuous skeletons were constructed and their basis width histograms were calculated with the radius step of 0.5 pixel.

For the same fonts the images of the characters were obtained in a lower resolution, so that the height of letter H was 100 and 70 pixels. For these

characters, width diagrams also were built. Step radius in the calculation was 0.05 and 0.035 pixels, respectively. These diagrams were normalized so that they could be compared with the diagrams of reference font characters. Normalization was done by stretching the diagrams 10 times along the x-axis and 100 times along the y-axis and 14.29 times along the x-axis and 204.08 times along the y-axis for low resolutions of 100 and 70 pixels respectively. As a result, all the normalized diagrams used the same set of radius values.

Creating of the skeletons and the calculation of width diagrams (for 52 glyphs of 1848 fonts) took in total less than 4 minutes on the computer with Intel® Core i5™ processor and 6GB of RAM

Further, for each font images of the 1000 common English words, random 30% of which were converted to upper case, were composed from the letters in low resolution. These images were used as the test set. Next, the diagrams of the letters on test images were compared with the diagrams of reference images in L_1 metric. As an integral font similarity metric we use a linear combination of distances between all characters present in the word. The coefficients of the linear form for each word were obtained by training on the entire set of test fonts. In the experiment, we calculated the distances for 52 letters between all pairs of 1848 typefaces, which took 18 minutes, and 1000 times trained the linear form, which took 32 minutes. This means that the time of the request – checking the typeface in the basis of the references – is 2 seconds and most of this time is spent to training of the linear form.

The experimental results showed that the font recognition accuracy by one word at the resolution of 100 was 91%, and at a resolution of 70 – more than 81%. Using the imaginary word containing all 52 characters we achieved the accuracy of 97% and 95% respectively.

Thus, the experiment confirmed the efficiency of the proposed method and showed its efficiency on the practical task of comparing a large number of images (1848×1848×52) with a fairly high recognition quality.

9 CONCLUSION

The proposed approach opens up new possibilities for the use of highly efficient computational geometry algorithms in image analysis and shape recognition. The continuous model of width of polygonal figures on the basis of the disk cover allowed to make the decomposition of the original

problem and reduce the computation to simple geometric calculations.

The developed algorithm is the first to provide accurate analytical representation of the width distribution function of a polygonal figure. Raster objects approximation with polygonal figures makes it possible to use the method in the analysis and recognition of images. The high efficiency of the proposed method allows to compare and measure the similarity of figures by their width in real-time computer vision systems.

ACKNOWLEDGEMENTS

The work was funded by Russian Foundation of Basic Research grant No. 14-01-00716.

REFERENCES

- Maragos P., 1989. Pattern Spectrum and Multiscale Shape Representation. In *IEEE Trans. On Pattern Analysis and Machine Intelligence*, Vol. 11, №7, pp. 701–716.
- Serra J., 1982. *Image Analysis and Mathematical Morphology*, London: Academic Press.
- Ramirez-Cortes, J.M., Gomez-Gil, P., Sanchez-Perez, G., Baez-Lopez, D., 2008. A Feature extraction method based on the pattern spectrum for hand shape biometry. In *Proc. World Congress on Engineering and Computer Science*.
- Vizilter Yu.V., Sidyakin S.V., 2012. Morphological spectra [in Russian]. In *Computer vision in control systems 2012. Proceedings of the scientific-technical conference, Moscow, 14–16 March, 2012*. Pp. 234–241.
- Vizilter Yu.V., Sidyakin S.V., 2015. Comparison of shapes of two-dimensional figures with the use of morphological spectra and EMD metrics. In *Pattern Recognition and Image Analysis, Vol. 25, No. 3*, pp. 365–372.
- Lomov N.A, Mestetskiy L.M, 2016. Area of the disk cover as an image shape descriptor. In *Computer Optics*, vol. 40(1), pp. 516-525.
- Mestetskiy, L., Semenov, 2008. Binary image skeleton continuous approach. *VISAPP 2008 - 3rd International Conference on Computer Vision Theory and Applications, Proceedings 1*, pp. 251-258.
- Yakupov E., Petrova I., Fridman G., Korolkova A., Levin B., 2015. *PARATYPE Originals – Digital Typefaces*. Moscow, 2015.